

Na⁺/H⁺ exchanger-1 reduces podocyte injury caused by endoplasmic reticulum stress via autophagy activation

Zhe Feng^{1,3}, Li Tang^{1,3}, Lingling Wu^{1,2}, Shaoyuan Cui¹, Quan Hong¹, Guangyan Cai¹, Di Wu¹, Bo Fu¹, Ribao Wei¹ and Xiangmei Chen¹

Podocyte injury has a critical role in the pathogenesis of proteinuria. Induction of endoplasmic reticulum (ER) stress is thought to lead to podocyte injury; however, no effective strategy for reducing ER stress-induced injury has been identified. We investigated specific mechanisms for reducing podocyte injury caused by ER stress. We found that the induction of ER stress in podocytes was related to cytoskeleton injury and increased proteinuria, which was associated with autophagy activation and downregulation of Na⁺/H⁺ exchanger-1 (NHE-1) in the rat model of passive Heymann nephritis. Using mouse podocyte cells (MPCs), we showed that ER stress could lead to podocyte injury accompanied by autophagy activation, and the disturbance of autophagy aggravated cytoskeleton loss under conditions of ER stress. The balance between autophagy activation and ER stress was critical to podocyte survival, in which the efficiency of autophagy could have a pivotal role. Strikingly, the overexpression and small interfering RNA knockdown of NHE-1 results suggested that NHE-1 exerts a protective effect by reducing the loss of synaptopodin in MPCs exposed to ER stress. This protective mechanism involves NHE-1 activation of autophagy via the PI3K/Akt pathway to reduce ER stress injury in podocytes. This mechanism may provide a new pathway to prevent podocyte injury.

Laboratory Investigation (2014) **94**, 439–454; doi:10.1038/labinvest.2014.4; published online 24 February 2014

KEYWORDS: autophagy; ER stress; glomerular disease; NHE-1; PHN; podocyte injury

Glomerular podocytes are highly specialized cells with cell bodies, major processes, and foot processes interlinked by slit diaphragms.¹ Podocyte injuries occur in many forms of human and experimental glomerular diseases, and lead to proteinuria.^{2–4}

Previous studies have suggested a role for endoplasmic reticulum (ER) stress induction in podocytes using models of membranous nephropathy (Heymann nephritis)^{5,6} and minimal-change nephrotic syndrome (puromycin nephrosis).⁷ Moderate stress in the ER triggers many rescue responses, including an unfolded protein response and ER-associated degradation.⁸ On the other hand, excessive or long-term exposure to ER stress induces impaired formation of the slit diaphragm complex and its associated lipid rafts as well as actin cytoskeleton abnormalities.⁹ However, the regulatory

mechanisms that determine the fate of the cell (cell survival or cell death) in response to ER stress are unclear.

Autophagy is a major homeostatic and quality control mechanism for maintaining cellular integrity, and is responsible for the bulk degradation of long-lived cytosolic proteins and organelles.^{10,11} Unlike proteasomal degradation, autophagic degradation is thought to be largely nonspecific,¹² but is frequently activated in response to an adverse environment or stress.^{13,14} Podocyte autophagy has been observed *in vitro*,¹⁵ in mice,¹⁶ and in human renal biopsies;¹⁷ autophagy occurs at a markedly higher level in podocytes than in other renal cells, indicating that it has a critical role in glomerular maintenance and function. Studies using the human neuroblastoma cell line¹⁸ have shown that autophagy is activated to enhance cell survival after ER stress, and disturbance of autophagy

¹State Key Laboratory of Kidney Diseases (2011DIV00088), Department of Nephrology, Chinese PLA Institute of Nephrology and Key Lab, Chinese PLA General Hospital, Beijing, China and ²Medical College, NanKai University, Tianjin, China

Correspondence: Professor X Chen, MD, PhD, State Key Laboratory of Kidney Diseases (2011DIV00088), Department of Nephrology, Chinese PLA Institute of Nephrology and Key Lab, Chinese PLA General Hospital, 28 Fuxing Road, Beijing 100853, China.

E-mail: xmchen301@126.com

³These authors contributed equally to this work.

Received 15 July 2013; revised 14 December 2013; accepted 30 December 2013

renders cells vulnerable to ER stress. Other studies have shown that autophagy is responsible for nonapoptotic cell death.^{19–21} However, the functional significance of autophagy of podocytes is unknown.

Na⁺/H⁺ exchanger-1 (NHE-1) is ubiquitously expressed in the plasma membrane of epithelial cells, including podocytes.^{22,23} In addition to its role in the maintenance of intracellular pH and volume, NHE-1 maintains cell morphology and structure; the juxtamembrane domain is anchored to the cytoskeleton and facilitates cytoskeleton rearrangement.^{23,24} The NHE-1/ERM/PI3K/Akt pathway regulates cell survival and apoptosis²³; similarly, autophagy activity is related to PI3K/Akt activity.²⁵ Therefore, we hypothesize that NHE-1 reduces podocyte injury via activation of autophagy.

In this study, we found that ER stress and autophagy in podocytes were related to increased proteinuria in a rat model of passive Heymann nephritis (PHN). We demonstrated that ER stress in podocytes induced cytoskeleton loss and recombination in conditionally immortalized mouse podocyte cells (MPCs). Disturbance of autophagy rendered cells vulnerable to ER stress. NHE-1 reduced podocyte injury by activating autophagy via PI3K/Akt pathway. This protective mechanism involving NHE-1 represents a new target for ameliorating podocyte injury caused by ER stress.

MATERIALS AND METHODS

Reagents

Cell culture media and supplements were obtained from Invitrogen. Tunicamycin (Tm), acridine orange (AO), DAPI, wortmannin, LY294002, E64d, and pepstatin A were purchased from Sigma-Aldrich. Primary antibodies were obtained from Sigma-Aldrich (anti-LC3 rabbit pAb; anti-NHE-1 rabbit pAb; anti-Actin mouse mAb), MBL (anti-LC3 mouse mAb), and Santa Cruz Biotechnology (anti-NHE-1 goat pAb; anti-calnexin goat pAb; anti-GRP94 rabbit pAb; anti-GRP78 rabbit pAb; anti-nephrin goat pAb; anti-synaptopodin goat pAb). Secondary antibodies were obtained from Jackson ImmunoResearch Laboratories. SignalSilence Akt small interfering RNA (siRNA) I (#6211) and SignalSilence Atg7 siRNA I (#6604) were obtained from Cell Signaling Technology.

Induction of PHN

Fx1A was isolated from Sprague–Dawley (SD) rat kidneys by sieving and ultracentrifugation, as described previously.²⁶ Rabbit anti-Fx1A was prepared by Beijing Biosynthesis Biotechnology. All experiments were performed in male SD rats (Beijing HFK Bio-Technology) with an initial body weight of 180–200 g. The rats had access to standard food and water *ad libitum* and were housed in a room with a 12-h dark–light cycle. Rats were then injected with anti-Fx1A serum (1 ml/100 g body weight; antibody titer: 1:250) into the caudal vein, followed by one further injection after 1 h. The control rats were injected with the same volume of normal saline. The rats were killed on 1, 7, 14, 21, and 28

days after injection for subsequent experiments (eight rats per group), and 24-h urinary albumin excretion was assessed by Coomassie Brilliant Blue G-250 staining.

Isolation of Rat Glomeruli

Rats were anesthetized and kidneys were removed. Then, kidneys were washed with cold physiological saline, the renal capsule was stripped, and the renal cortex was cut into pieces using scissors. Glomeruli were isolated by pressing minced kidneys through a 250- μ m sieve, followed by passage through a 106- μ m sieve and were collected from the top of a 75- μ m sieve. Tissue was sucked out from the third sieve and observed under a microscope. When only glomeruli and almost no tubular cells could be seen (glomerular purity > 95%), washes were discontinued and tissues were collected from this layer and transferred into centrifuge tubes. After centrifugation and discarding the supernatant, the precipitate containing isolated glomeruli was stored at –80 °C. These isolated glomeruli were subjected to western blotting.

pcDNA-NHE-1 Plasmid Construction and siRNA-NHE-1 Design

The cloning vector pIRES-EGFP, containing mouse NHE1 full cDNA, was kindly provided by Dr Tony Green (Cambridge Institute for Medical Research, University of Cambridge, UK). The eukaryotic expression vector pcDNA 3.1 was obtained from Invitrogen. NHE1 cDNA (2.5 kb) from the plasmid pIRES-EGFP-NHE-1 was inserted into the vector pcDNA 3.1 with *EcoRI* and *NheI* restriction endonucleases (Supplementary Figures 1A and B), which resulted in pcDNA-NHE-1, and this was sequenced by BGI. siRNAs against NHE-1 were designed by Shanghai GenePharma (Shanghai, China). Two siRNA-NHE-1-specific oligos: 5'-GAC CAA CUU AAU CAU UGA ATT-3' and 5'-UUC AAU GAU UAA GUU GGU CTT-3', and two control siRNA oligos: 5'-UUC UCC GAA CGU GUC ACG UTT-3' and 5'-ACG UGA CAC GUU CGG AGA ATT-3' were used.

Cell Culture and Transfection

Conditionally immortalized MPCs were kindly provided by Dr Peter Mundel (University of Miami, Miami, FL, USA) and were cultured as described previously.²⁷ In brief, MPCs were cultured in RPMI-1640 medium supplemented with 10% fetal calf serum. MPC cells were cultured at 33 °C (permissive conditions) for propagation and were shifted to 37 °C in γ -interferon-free medium for 7 days (non-permissive conditions) to induce differentiation. MPCs between passage 10 and 14 were used in all experiments.

Differentiated MPCs were transfected for 48 h with plasmids or siRNA using jetPRIME (Polyplus-transfection) as per the manufacturer's recommendation. Transfection efficiency was determined by immunofluorescence (Supplementary Figures 2A and B).

Immunofluorescence and Confocal Microscopy

MPCs were cultured to 70% confluence in special glass-bottom microwell dishes (MatTek). Immunofluorescence double staining was performed using a routine procedure.^{15,28} Images were obtained using a laser-scanning microscope (FV1000, Olympus).

Western Blotting

Western blotting was performed using a routine procedure. To demonstrate autophagy activation by light chain 3 (LC3)-II bands, cells were pretreated for the indicated period in the presence or absence of 2.5 $\mu\text{g}/\text{ml}$ Tm with lysosome inhibitors (10 mg/ml E64d and 10 mg/ml pepstatin A), and lysed in RIPA buffer (50 mM Tris-Cl (pH 7.6), 5 mM EDTA, 150 mM NaCl, 0.5% NP-40, and 0.5% Triton-X-100) that contained 1 mM sodium orthovanadate, 0.5 mM phenylmethylsulfonyl fluoride, and 1 $\mu\text{g}/\text{ml}$ each of leupeptin, aprotinin, and antipain. Protein concentration was measured using the Bradford assay. Isolated glomerulus protein (60–80 μg) or MPCs total protein (30–40 μg) was subjected to SDS-PAGE and then transferred to a membrane. The membrane was blocked with 5% skim milk, probed with a primary antibody overnight at 4 °C, and incubated with a horseradish peroxidase-conjugated secondary antibody. Proteins were detected by chemiluminescence using the ECL reagent (Pierce, Rockford, IL, USA). Proteins were visualized with an enhanced chemiluminescence system. Densitometry was performed using AlphaImage2000 (Alpha Innotech, USA) analysis software. β -actin was used as the normalization control.

Terminal Deoxynucleotidyl Transferase-Mediated Biotinylated UTP Nick End-Labeling Analysis

Four micron thick slides of kidney tissue were obtained from paraffin-embedded tissue and MPCs were cultured to 70% confluence in special glass-bottom microwell dishes. Terminal deoxynucleotidyl transferase-mediated biotinylated UTP nick end-labeling (TUNEL) staining was performed using the In Situ Cell Death Detection Kit, POD (Roche, Switzerland).

GFP-LC3B Overexpression and Autophagy Detection

MPCs were cultured to 50% confluence in special glass-bottom microwell dishes, and then transfected with GFP-LC3B plasmid (a gift from Dr Christian Münz, Rockefeller University, New York, USA) using jetPRIME for 36 h. The GFP-LC3B-transfected cells were used for experimental conditions. Microphotographs of GFP-LC3B fluorescence were obtained using a confocal microscope.

Evaluation of Autophagic Vacuoles by AO

MPCs were cultured to 70% confluence in special glass-bottom microwell dishes. At the end of the incubation period, MPCs were treated with 5 $\mu\text{g}/\text{ml}$ AO in serum-free medium for 15 min. Subsequently, the cells were washed three times with PBS and examined by confocal microscopy. Acidic autophagic vacuoles were quantified as the number of

red granules per cell. A minimum of 100 cells was counted for each variable.

Statistical Analysis

Data are expressed as means \pm s.d. Statistical analyses were performed using the SPSS ver. 10.0 software package (SPSS, USA). Differences were evaluated by analysis of variance. $P < 0.05$ denotes a statistically significant difference.

RESULTS

Podocyte Injury is Closely Related to ER Stress Activation in PHN Rats

We used the PHN rat model to explore the relationship between ER stress-induced podocyte injury and proteinuria *in vivo*. To induce PHN, SD rats (180–200 g) were injected with commercially available rabbit anti-Fx1A IgG antibody. A fluorescence assay showed that rabbit IgG was deposited granularly along the glomerular capillary walls in rats with PHN, and no rabbit IgG was observed in the glomerulus in control rats (Figure 1a). Using a Coomassie Brilliant Blue G-250 assay to detect urinary albumin, a gradual increase in the level of proteinuria was observed from day 1 to 14 after injection in PHN rats, and levels of proteinuria 14 days after injection reached a peak (26.69 ± 8.68 mg per 24 h on day 14 vs 3.29 ± 0.77 mg per 24 h on day 0; $P < 0.01$; eight rats per group; Figure 1b). The level of proteinuria in normal SD rats is < 5 mg per 24 h.²⁶

To verify podocyte injury in the kidneys of PHN rats, we examined the expression of synaptopodin (a protein marker of podocytes) by western blotting of isolated glomerular protein. Compared with the control group, downregulated synaptopodin expression in PHN rats was observed on day 7, and showed the largest decrease on day 14 (Figures 2a and b). Similar to the increase in proteinuria, the expression of GRP94 and GRP78 (markers of ER stress) was clearly increased on day 14 after injection in PHN rats. This demonstrates that ER stress is activated and is related to proteinuria and podocyte injury *in vivo*. Furthermore, compared with controls, we found significantly increased expression levels of calnexin protein, an ER stress marker,²⁸ in PHN rats on day 14, and decreased levels of nephrin and synaptopodin proteins (podocyte markers) and intermittent localization along the glomerular capillary walls and in PHN rats on day 14 (Figure 2c). At the same time, we found podocyte apoptosis, assessed by TUNEL staining, is significantly increased on day 14 (Figure 2d). Therefore, during the PHN period, ER stress activation is closely related to podocyte injury and increased proteinuria.

Podocyte Injury is Related to Autophagy Activity and Decreased NHE-1 Protein in PHN Rats

Autophagy activation is characterized by the presence of LC3 conversion (from LC3-I to LC3-II). The amount of LC3-II is closely correlated with the number of autophagosomes, serving as a good indicator of autophagosome formation.^{29,30}

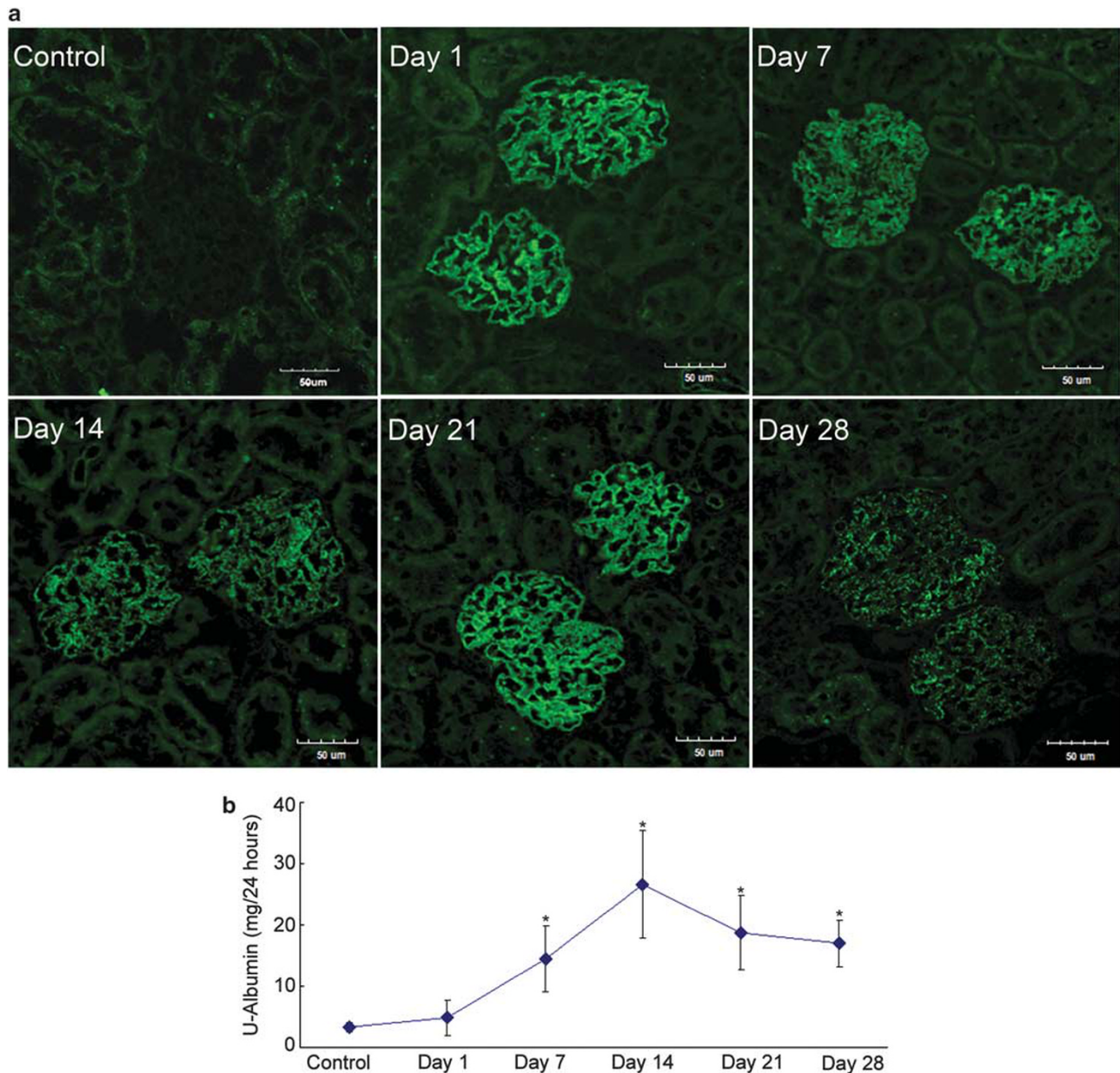
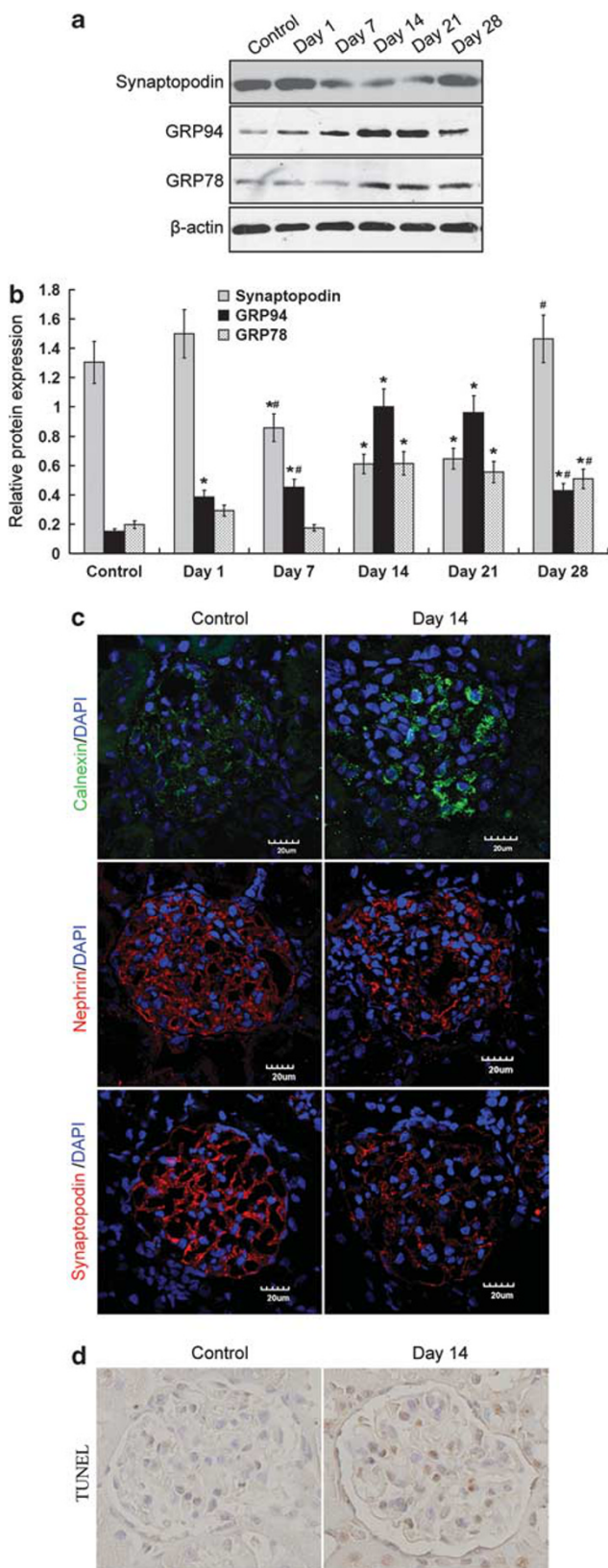


Figure 1 Construction of a stable passive Heymann nephritis (PHN) disease rat model using anti-Fx1A antibody-induced representative immunofluorescent IgG deposits in glomeruli and long-lasting severe proteinuria. **(a)** The antibody was intravenously injected at a volume of 1.0 ml per 100 mg at days 1, 7, 14, 21, and 28. Cryosections were stained with goat anti-rat IgG-fluorescein isothiocyanate. Glomeruli from control rats were negative, whereas glomeruli from day-1 PHN model rats showed intense, granular capillary wall staining, original magnification $\times 600$. Scale bar = 50 μm . **(b)** Urine samples (24 h) collected from control rats and PHN model rats on days 1, 7, 14, 21, and 28 were analyzed for urinary albumin content using Coomassie Brilliant Blue G-250. Data are presented as means \pm s.e.m. ($n=8$). * $P<0.01$ vs control.

Using western blotting with anti-LC3 antibody, we found that the ratio of LC3-II/LC3-I was significantly increased in isolated glomerular tissues from PHN rats on day 14 compared with that in control rats (Figures 3a and b). Double immunofluorescence staining showed that LC3 expression (green) was colocalized with synaptopodin, indicating that autophagy was activated in podocytes. Concomitant with LC3 activation, decreased expression of synaptopodin and intermittent expression along the glo-

merular capillary walls in PHN rats was observed on day 14 compared with controls (Figure 3c). Furthermore, NHE-1 protein decreased in a time-dependent manner from days 1 to 21 after injection in glomerular tissues from PHN rats (Figures 4a and b). Immunofluorescence staining showed that NHE-1 expression in the glomerulus was lower on day 14 than that in control rats (Figure 4c). These results indicate that podocyte injury is related to autophagy activity and decreased NHE-1 protein in podocytes from PHN rats.



ER Stress Activates Autophagy and Damages the Podocyte Cytoskeleton

Next, we investigated the mechanism of podocyte injury using Tm to induce ER stress in MPCs. Western blotting showed increased expression levels of GRP94 and GRP78 in differentiated Tm-treated MPCs in a time-dependent manner, which reached their peak levels at the 10-h time point (Figures 5a and b). Before Tm stimulation, immunofluorescence assays (Figure 5c) showed that calnexin (green) was slightly expressed in the cytoplasm and synaptopodin (red) showed arborization accompanied by large macula. After adding Tm, calnexin accumulated in the cytoplasm, and cytoskeleton arborization of synaptopodin disappeared, and podocyte apoptosis increased. These results indicate that ER stress can induce podocyte injury.

Tm stimulated a decrease in synaptopodin protein and an increase in the ratio of LC3-II/LC3-I (Figures 5d and e). To monitor autophagy, differentiated MPCs were transiently transfected with GFP-LC3B, an autophagosome marker. As a convenient way to monitor autophagy, LC3B with a fluorescent protein (GFP-LC3) has been used to monitor autophagy through indirect immunofluorescence or direct fluorescence microscopy, measured as an increase in punctate LC3 or GFP-LC3.³¹ After adding Tm, transfected cells displayed a conversion from dispersed to granular accumulation in the cytoplasm (Figure 5f), suggesting that ER stress induced autophagosomes in podocytes. To further quantify autophagosome formation, we used AO staining to enumerate intracellular red granules as a measure of acidic autophagic vacuoles in podocytes. Figures 5f and g show a considerable increase in the number of autophagic vacuoles when stimulated by Tm (6.08 ± 3.03 vs 40.53 ± 4.67 per cell; $P < 0.01$; $n = 100$). These results suggest that ER stress can activate autophagy in podocytes; however, whether autophagy activation is a protective effect or a cell injury factor requires further investigation.

Western blotting (Figures 5d and e) and immunofluorescence (Figure 5f) showed that Tm decreased NHE-1 expression in podocytes, suggesting that ER stress inhibits NHE-1 expression.

Figure 2 Endoplasmic reticulum (ER) stress, decreased nephrin and synaptopodin expression, and cell apoptosis during passive Heymann nephritis (PHN). (a, b) The expression of synaptopodin (a podocyte marker) and GRP94/GRP78 (ER stress markers) was determined by western blot analysis at various time points in PHN rats, $*P < 0.01$ vs control, $^{\#}P < 0.01$ vs day 14. (c) Confocal microscopy analysis of cryosections from PHN rat kidney tissue in controls and on day 14 confirmed expression of calnexin (green, an ER stress marker), nephrin, and synaptopodin (red, podocyte injury markers), original magnification $\times 600$. Scale bar = 20 μm . The nucleus is stained blue. (d) Use of terminal deoxynucleotidyl transferase-mediated biotinylated UTP nick end-labeling (TUNEL) staining to measure the apoptosis of podocytes in the PHN rat kidney tissue of the day 14 and the controls' original magnification $\times 600$. The experiments was repeated three times in separate kidneys from different rats.

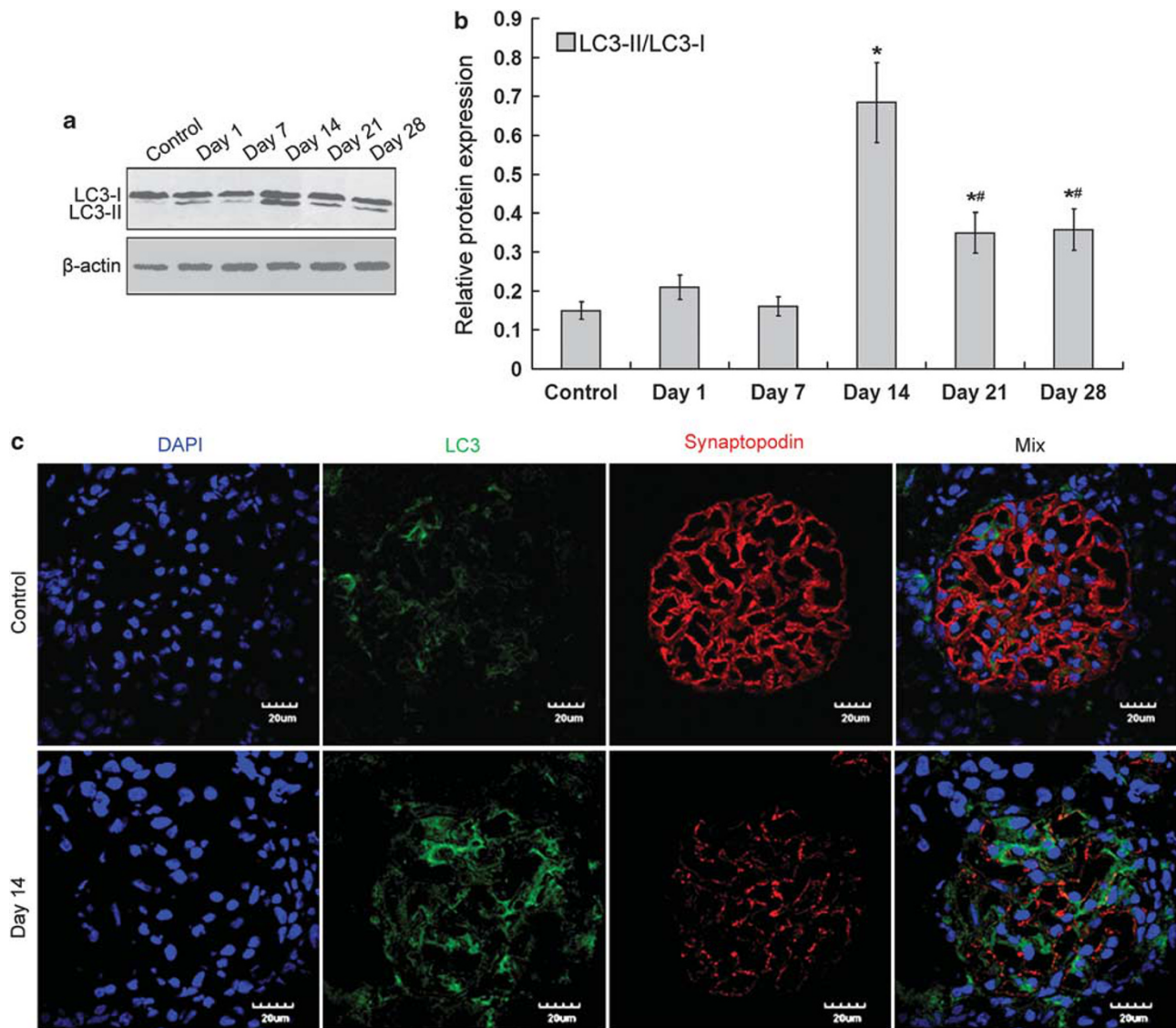


Figure 3 Upregulation of autophagy in podocytes during passive Heymann nephritis (PHN). (**a**, **b**) The extent of light chain 3 (LC3) conversion (from the LC3-I form to LC3-II form) was determined by western blot analysis with mouse anti-LC3 monoclonal antibody at various time points in PHN rats, * $P < 0.01$ vs control, ** $P < 0.01$ vs day 14. (**c**) Confocal microscopy analysis of cryosections from PHN rat kidney tissue in control and in PHN rats on day 14 confirmed expression of LC3 (green, an autophagy marker) and synaptopodin (red, a podocyte marker). LC3 is colocalized with synaptopodin, original magnification $\times 600$. Scale bar = $20 \mu\text{m}$. The nucleus is stained blue. The experiment was repeated three times in separate kidneys from different rats.

Inhibition of Autophagy Aggravates Injury of Podocytes due to ER Stress

To investigate the role of autophagy in podocytes, we used wortmannin and the siRNA of ATG7 to inhibit autophagy.³² The extent of LC3 conversion (LC3-II/LC3-I) was inhibited after the addition of 50 nM wortmannin for 10 h, but GRP94 expression was higher than that in untreated MPCs or Tm-treated MPCs alone (Figure 6a). Then, MPC cells were transfected with siRNA-ATG-7 or negative control siRNA and stimulated by Tm for 10 h; the ratios of LC3-II/LC3-I was decreased and GRP94 expression was higher in the presence

of siRNA-ATG-7 compared with cells transfected with negative control siRNA (siRNA-con; Figure 6b). As shown by AO staining, acidic autophagic vacuoles were decreased in Tm-treated MPCs with addition of wortmannin (9.85 ± 4.60 per cell) or siRNA-ATG-7 (13.26 ± 7.89 per cell) compared with those in Tm-treated MPCs alone (40.43 ± 4.96 per cell) and with addition of siRNA-con (35.48 ± 7.26 per cell; * $P < 0.01$; $n = 100$; Figures 6c and d). When autophagy was inhibited after adding 50 nM wortmannin or siRNA-ATG-7, increased calnexin expression, decreased synaptopodin expression (Figures 6e and f), and increased podocyte

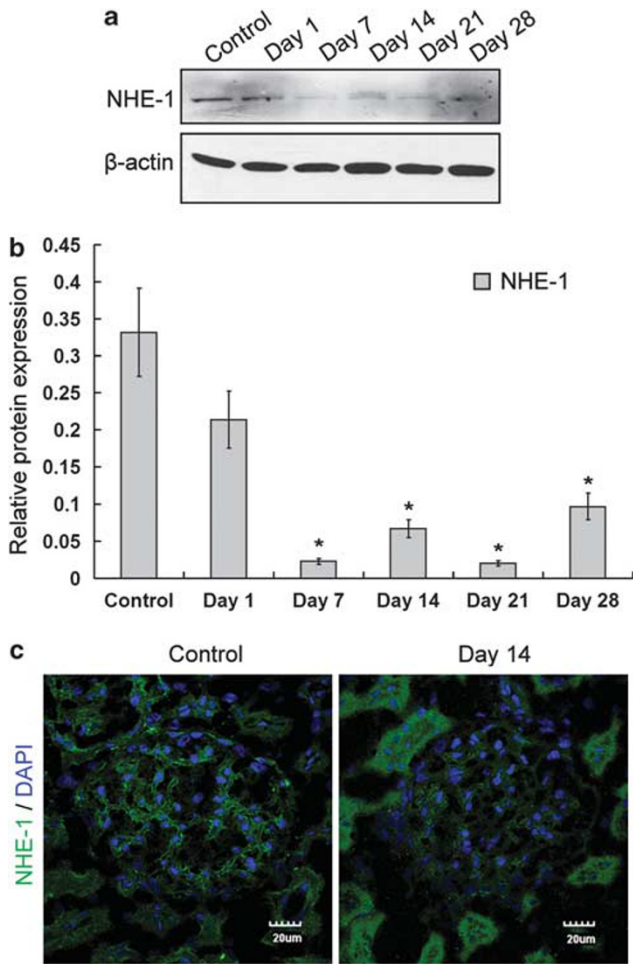


Figure 4 Downregulation of Na^+/H^+ exchanger-1 (NHE-1) during passive Heymann nephritis (PHN). **(a, b)** NHE-1 expression was measured by western blot analysis using anti-NHE-1 antibody at various time points in isolated glomerular tissues from PHN rats, $*P < 0.01$ vs control. **(c)** Confocal microscopy analysis of cryosections from PHN rat kidney tissue and controls on day 14 confirmed NHE-1 expression (green), original magnification $\times 600$. Scale bar = $20 \mu\text{m}$. The nucleus is stained blue. The experiment was repeated three times in separate kidneys from different rats.

apoptosis (Figure 6g) were observed. These results show that ER stress-induced podocyte injury is aggravated when autophagy is inhibited.

We used LC3/synaptopodin double fluorescence staining to obtain direct evidence for inhibition of autophagy and podocyte injury. Figure 6f shows decreased LC3 and synaptopodin expression with addition of wortmannin or siRNA-ATG-7 compared with that in cells treated with Tm alone. These results demonstrate that autophagy protects podocytes from ER stress.

NHE-1 Reduces Injury of Podocytes Induced by Tm Via Activation of Autophagy

After showing that ER stress was accompanied by a reduction in NHE-1 during the progression of PHN, we next investigated whether NHE-1 regulates ER stress. To address this, we constructed the plasmid pcDNA-NHE-1 (Supplementary Figure 1) and siRNA-NHE-1 oligonucleotide, and transiently transfected them into differentiated MPCs (Supplementary Figures 2A–D).

Overexpression of NHE-1 downregulated GRP94 and GRP78 protein expression, as shown by western blotting (Figures 7a and b) and calnexin fluorescence staining (Figure 7c). However, siRNA-NHE-1 inhibition of NHE-1 resulted in the upregulation of GRP94 protein expression (Figures 8a and b), indicating that NHE-1 negatively regulates ER stress. Overexpressed NHE-1 in MPCs resulted in increased GFP-LC3B dot formation compared with that in the nontransfected group after Tm stimulation (Figure 8c); however, NHE-1-deficient MPCs showed little GFP-LC3B dot formation. Western blotting showed an increased ratio of LC3-II/LC3-I in MPCs with NHE-1 overexpression and a decreased ratio in NHE-1-deficient MPCs compared with that in the control and transfected control groups (Figures 8a and b). As seen by AO staining (Figure 8c), acidic autophagic vacuoles accumulated in MPCs with NHE-1 overexpression compared with those in nontransfected MPCs after Tm stimulation (58.02 ± 9.58 vs 40.33 ± 9.78 per cell; $P < 0.01$), and were inhibited in NHE-1-deficient MPCs (13.78 ± 6.09

Figure 5 Downregulation of synaptopodin expression, increased apoptosis and autophagy activity, and decreased Na^+/H^+ exchanger-1 (NHE-1) expression in tunicamycin (Tm)-treated differentiated mouse podocyte cells (MPCs). **(a, b)** GRP94 and GRP78 expression levels were measured by western blot analysis at various time points in Tm ($2.5 \mu\text{g}/\text{ml}$)-treated differentiated MPCs. Data are representative of three independent experiments, $*P < 0.01$ vs control. **(c)** Immunostaining results of calnexin (an endoplasmic reticulum (ER) stress marker, green) and synaptopodin (red) are shown by confocal microscopy with or without Tm ($2.5 \mu\text{g}/\text{ml}$ for 10 h) in differentiated MPCs, scale bar = $20 \mu\text{m}$. The nucleus was stained blue. The apoptosis of MPCs with or without Tm ($2.5 \mu\text{g}/\text{ml}$ for 10 h) was measured by using terminal deoxynucleotidyl transferase-mediated biotinylated UTP nick end-labeling (TUNEL) staining. The experiments were repeated three times. **(d, e)** Synaptopodin expression and the extent of light chain 3 (LC3) conversion were determined by western blot analysis. **(f)** Autofluorescence of GFP-LC3 in the presence or absence of $2.5 \mu\text{g}/\text{ml}$ Tm-treated differentiated MPCs. Cells were transiently transfected with GFP-LC3 for 48 h. Images were recorded digitally to indicate the change in GFP-LC3B (showing granules) distribution pattern. Punctate LC3 staining was characteristic of autophagosome formation. Formation of acidic autophagic vacuoles (red granules) is shown by acridine orange (AO). Differentiated MPCs with or without Tm ($2.5 \mu\text{g}/\text{ml}$ for 10 h) were incubated with $5 \mu\text{g}/\text{ml}$ AO in serum-free medium for 15 min. AO was removed and fluorescent micrographs were obtained using a confocal microscope. Acidic autophagic vacuoles were quantified, and **(g)** data are presented as the number of red granules per cell. A minimum of 100 cells was counted. $*P < 0.01$ compared with controls. NHE-1 expression was determined by western blot analysis **(d, e)** and immunofluorescence staining **(f)**. Data are representative of three independent experiments, scale bar = $20 \mu\text{m}$.

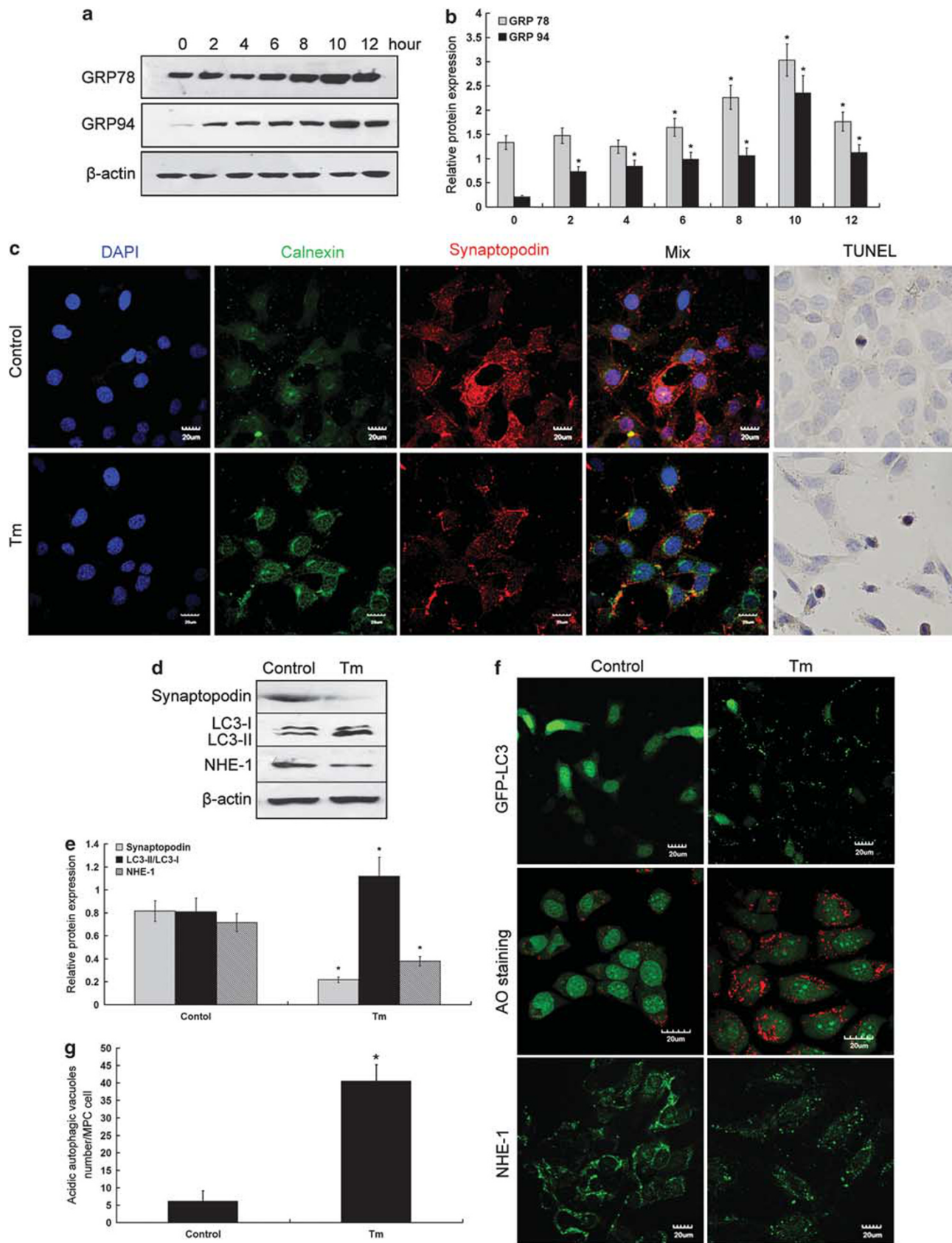


Figure 5 For caption see page 445.

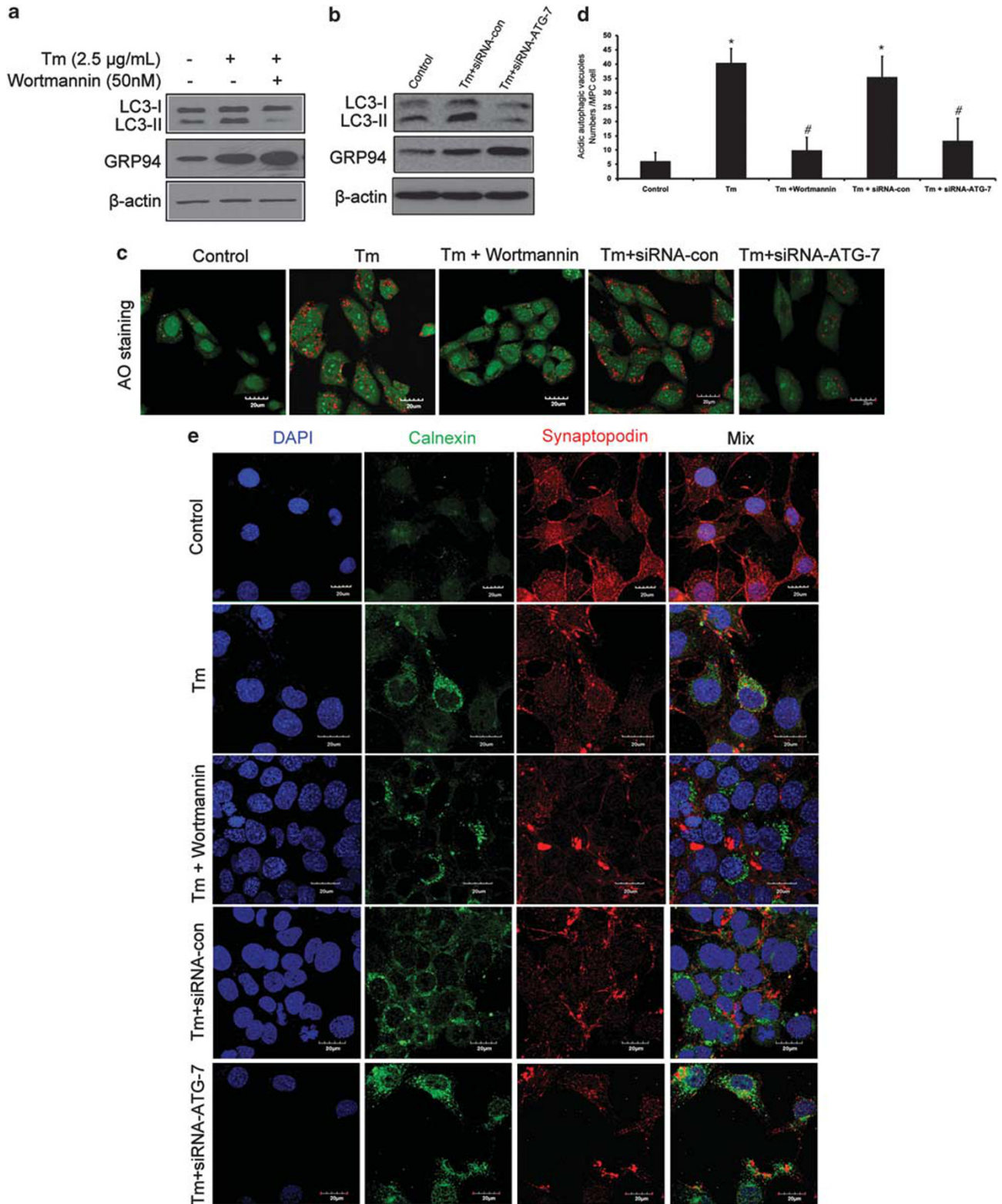
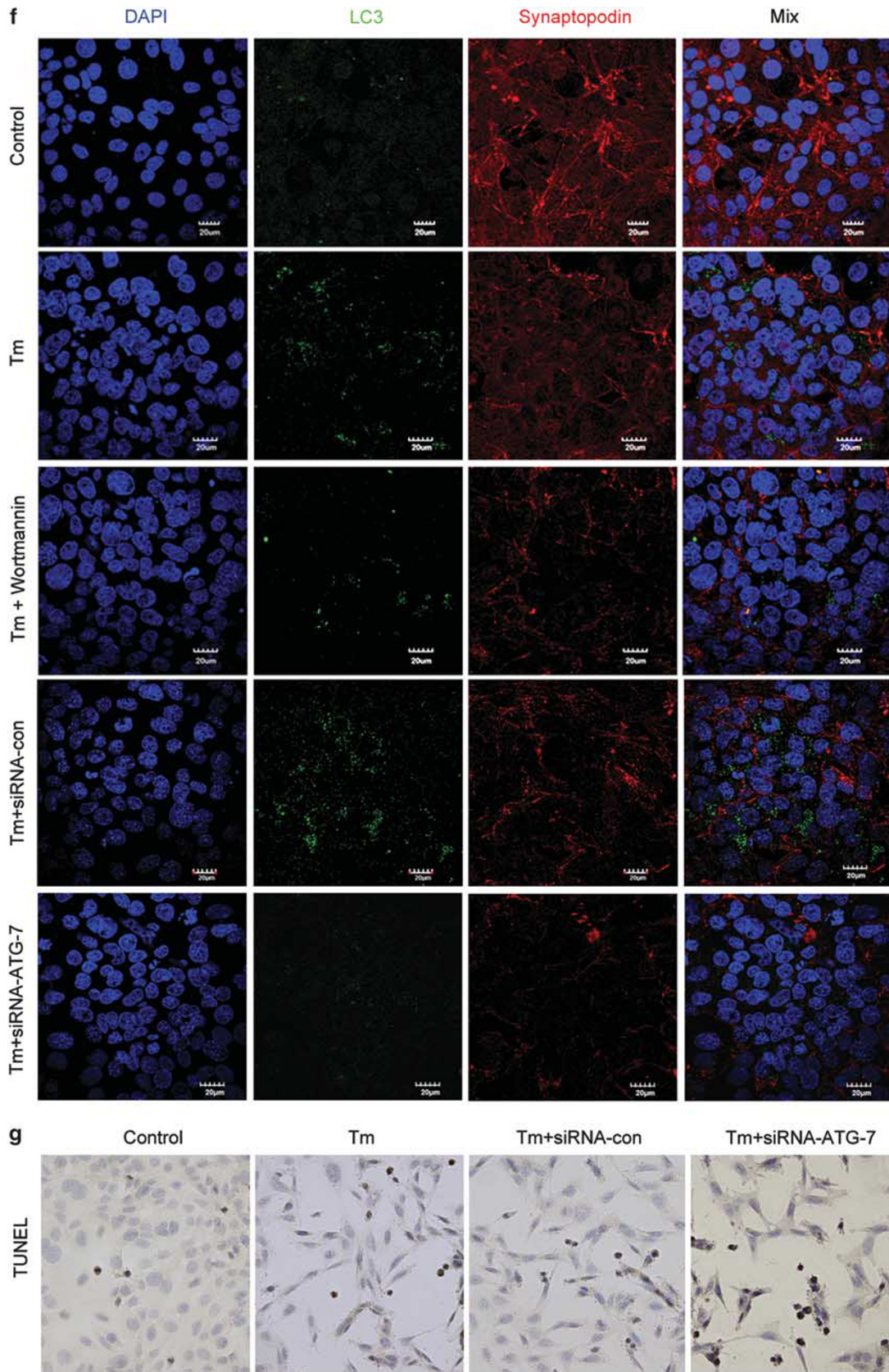


Figure 6 Continued.



per cell; $P < 0.01$ vs Tm group). These results demonstrated that NHE-1 can upregulate autophagy and inhibit ER stress.

By LC3/synaptopodin double fluorescence staining and TUNEL assay, we showed that overexpression of NHE-1 resulted in accumulated LC3 dot formation in the cytoplasm with no loss of synaptopodin and decreased podocyte apoptosis, which reduced podocyte injury. However, NHE-1 deficiency inhibited GFP-LC3B dot formation and aggravated the loss of synaptopodin (Figure 8d) and increased podocyte

apoptosis (Figure 8e). These results indicate that NHE-1 reduces podocyte injury induced by ER stress via activation of autophagy.

NHE-1 Activates Autophagy Via Activating PI3K/Akt Pathway

To determine the pathway by which NHE-1 regulates autophagy activation, we employed PI3K/Akt inhibitors (wortmannin and LY294002), siRNA-Akt, and siRNA-ATG-7.

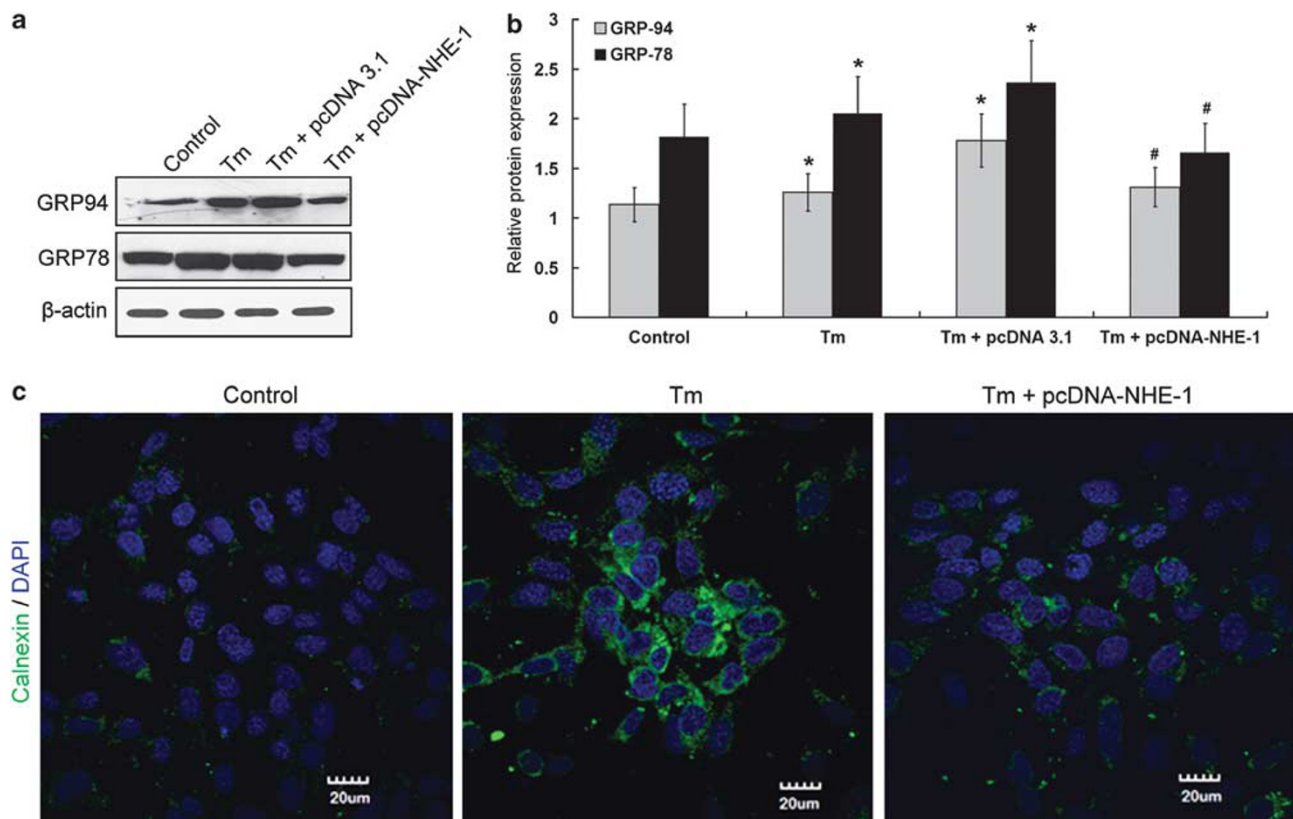
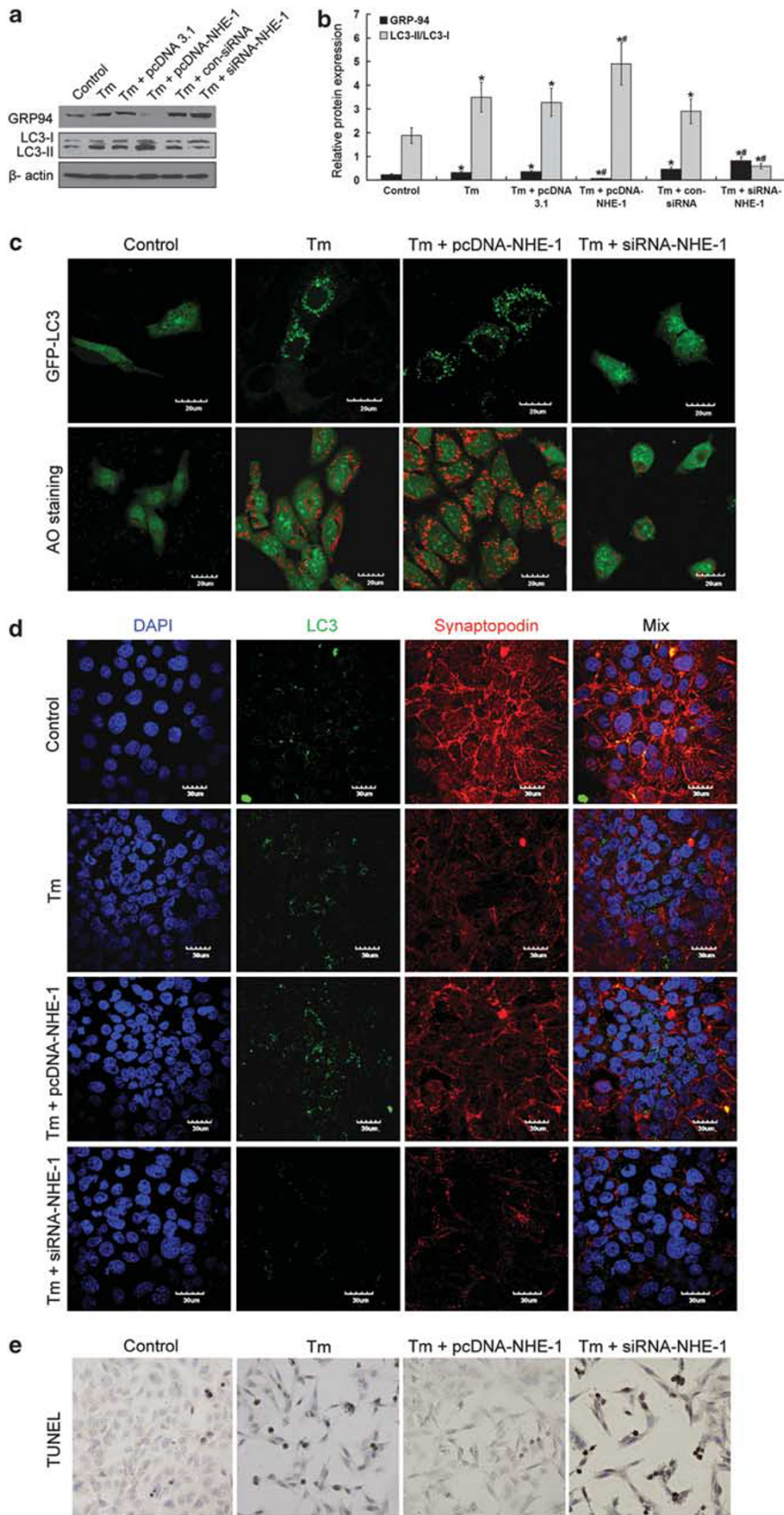


Figure 7 Overexpression of Na^+/H^+ exchanger-1 (NHE-1) inhibits the endoplasmic reticulum (ER) stress in tunicamycin (Tm)-treated differentiated mouse podocyte cells (MPCs). (a, b) The expression of GRP78 and GRP94 was determined by western blot analysis in controls, Tm-treated, Tm + pcDNA 3.1 vector, and Tm + pcDNA-NHE-1 vector-treated differentiated MPCs. Tm (2.5 μ g/ml) was added to differentiated MPCs after the pcDNA 3.1 vector and pcDNA-NHE-1 were transfected for 48 h. Data are representative of three independent experiments, * $P < 0.01$ vs control, # $P < 0.01$ vs Tm group. (c) Confocal immunostaining results of DAPI (blue)/calnexin (green) are shown in controls, Tm (2.5 μ g/ml)-treated, Tm + pcDNA 3.1 vector, and Tm + pcDNA-NHE-1 vector-treated differentiated MPCs, scale bar = 20 μ m. This experiment was repeated three times.

Figure 6 Inhibition of autophagy enhances the endoplasmic reticulum (ER) stress-induced injury in tunicamycin (Tm)-treated differentiated mouse podocyte cells (MPCs). (a) The extent of light chain 3 (LC3) conversion and GRP94 expression was determined by western blot analysis in controls and Tm (2.5 μ g/ml)-treated differentiated MPCs with or without wortmannin (50 nM). (b) The extent of LC3 conversion and GRP94 expression was determined by western blot analysis in controls and Tm (2.5 μ g/ml)-treated differentiated MPCs with control small interfering RNA (siRNA; siRNA-con) or siRNA-ATG-7. Data are representative of three independent experiments. (c, d) Formation of acidic autophagic vacuoles (red granules) in controls and Tm (2.5 μ g/ml)-treated differentiated MPCs with wortmannin (50 nM), siRNA-con, or siRNA-ATG-7 are shown by acridine orange (AO). Acidic autophagic vacuoles were quantified, and data are presented as the number of red granules per cell. A minimum of 100 cells was counted. * $P < 0.01$ vs control, # $P < 0.01$ vs Tm group. (e, f) Confocal immunostaining results of DAPI (blue)/calnexin (green)/synaptopodin (red; e) and DAPI (blue)/LC3 (green)/synaptopodin (red; f) are shown in controls and Tm (2.5 μ g/ml)-treated differentiated MPCs with wortmannin (50 nM), siRNA-con, or siRNA-ATG-7. Scale bar = 20 μ m. This experiment was repeated three times.



Differentiated MPCs were transfected with pcDNA 3.1 and pcDNA-NHE-1 plasmids, which were then stimulated by Tm with or without wortmannin (50 nM) and LY294002 (50 nM) for 10 h. LC3B, Akt, and pAkt proteins were detected by western blotting. Upregulated expression of pAkt and LC3-II/LC3-I ratio was found in MPCs overexpressing NHE-1, which was abolished after addition of wortmannin and LY294002; no change in total Akt was observed (Figures 9a and b). AO staining showed a decreased number of acidic autophagic vacuoles per MPC cell in the Tm + pcDNA-NHE-1 + wortmannin or LY294002 group compared with that in the Tm + pcDNA-NHE-1 group ($P < 0.01$, Figures 9c and d). These results showed that both inhibitors inhibited NHE-1-induced autophagy in podocytes.

To investigate whether NHE-1 could regulate autophagy via the PI3K/Akt pathway, NHE-1-overexpressing MPC cells were transfected with SignalSilence Akt siRNA I or SignalSilence ATG-7 siRNA I and stimulated by Tm for 10 h. Figures 9e and f show decreased synaptopodin expression and ratios of LC3-II/LC3-I in the presence of siRNA-Akt compared with cells transfected with the control (siRNA-con). These results indicate that NHE-1 exerted a protective effect on podocytes via the Akt autophagy pathway. Next, we used ATG-7 siRNA interference technology to interfere directly with autophagy (Figures 9g and b). We found that synaptopodin expression could not be upregulated in NHE-1-overexpressing MCP cells after Tm stimulation. Furthermore, no change in the total Akt was observed. These results suggest that Akt was the upstream signaling pathway of autophagy.

In this study, we demonstrated that NHE-1 exerts a protective effect against ER stress-induced podocyte injury by activating PI3K/Akt pathway.

DISCUSSION

Podocytes are terminally differentiated cells that cannot regenerate after injury. In most human glomerulopathies, cytoskeletal injuries and reparative mechanism failures promote persistent proteinuria and the development of glomerulosclerosis.³³ Adaptation reactions to persistent stress (eg, complement, viruses, drugs, and high glucose) are key for podocyte survival and functional maintenance. However, little is known about the molecular nature of the reparative mechanisms that defend podocytes against environmental

stress. This study suggests that ER stress in podocytes is responsible for causing an increase in proteinuria in PHN rats. The efficiency of autophagy appeared to be a direct determinant of the improvement of unfolding or misfolding of proteins due to ER stress. In addition to having a role in the maintenance of intracellular pH and volume, NHE-1 appears to regulate autophagy activation via PI3K/Akt pathway and reduce ER stress-induced injury in podocytes. This novel role of NHE-1 is a newly discovered pathway that ameliorates podocyte injury and decreases proteinuria during the course of glomerular disease.

Short-term induction of ER stress proteins by pretreatment with a subnephritogenic dose of adriamycin or Tm stimulation can protect podocytes from injury *in vivo*; however, a long exposure can induce pathological damage.^{34,35} In the PHN model, induction of ER stress proteins by injection of Fx1A was closely related to podocyte injury (including cytoskeleton injury and apoptosis) and increased proteinuria, which is consistent with other reports.^{5,6,36} Expression of ER stress proteins was accompanied by autophagy activation in podocytes. Furthermore, Tm induced expression of ER stress proteins *in vitro* and decreased the expression of podocyte cytoskeleton proteins (synaptopodin and nephrin) and increased podocyte apoptosis. Western blot detection of LC3-II expression, GFP-LC3B expression, and AO staining assays showed that induction of ER stress activated autophagy in differentiated podocytes. Autophagosome formation was inhibited by pharmacological inhibitors of PI3-kinases, including wortmannin and LY294002 and by ATG-7 siRNA interference technology (siRNA-ATG-7). During inhibition of autophagy, ER-stress protein expression was higher after Tm stimulation, indicating that autophagy inhibition enhances ER stress, aggravates the loss of synaptopodin, and induces apoptosis. Therefore, we speculate that autophagy activated during the PHN process results in scavenging of unfolded/misfolded proteins. The unfolded protein response is a classic mechanism in which cells mount a response to relieve ER stress, which reduces overall cellular protein synthesis, assists in protein folding, and promotes ER-associated degradation.³⁷ In addition to this protective mechanism, autophagy is also thought to regulate ER stress.¹⁸ Hartleben B *et al*²⁸ also reported that podocyte-specific deletion of autophagy led to a glomerulopathy in aging mice that was accompanied by an accumulation of oxidized and ubiquitinated proteins, ER stress, and

Figure 8 Na⁺/H⁺ exchanger-1 (NHE-1) reduces the endoplasmic reticulum (ER) stress-induced podocyte injury by promoting autophagy. (a, b) The expression of GRP94 and the extent of light chain 3 (LC3) conversion were determined by western blot analysis in differentiated mouse podocyte cells (MPCs) * $P < 0.01$ vs control, [#] $P < 0.01$ vs tunicamycin (Tm) group. (c) Autofluorescence of GFP-LC3 in differentiated MPCs. Cells were transiently transfected with NHE-1 vector or small interfering RNA (siRNA), followed by transfection with GFP-LC3 for 38 h. Tm was then added to cells for 10 h. Images were recorded digitally to indicate the change in GFP-LC3B (showing granules) distribution pattern, characteristic of autophagosome formation. Representative pictures are shown. Formation of acidic autophagic vacuoles (red granules) in differentiated MPCs are shown by acridine orange (AO). (d) Confocal immunostaining results of DAPI (blue)/LC3 (green)/synaptopodin (red) are shown, scale bar = 20 μm. (e) The apoptosis of podocytes was measured by terminal deoxynucleotidyl transferase-mediated biotinylated UTP nick end-labeling (TUNEL) staining. All experiments were as follows: cells were transiently transfected with pcDNA 3.1 vector (negative control), pcDNA-NHE-1 vector, con-siRNA (negative control), or siRNA-NHE-1 for 38 h. Tm (2.5 μg/ml) was then added to cells for 10 h. This experiment was repeated three times.

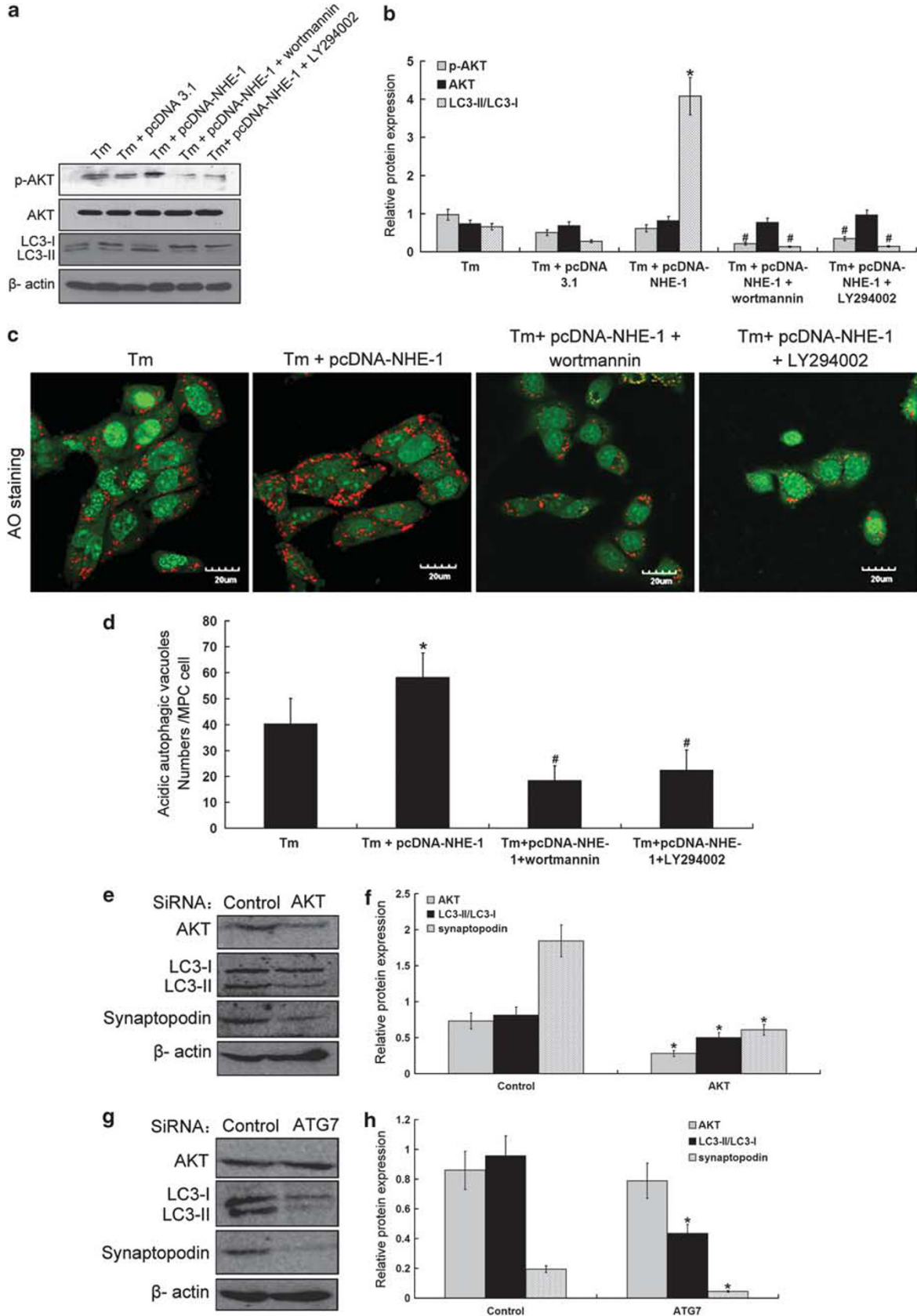


Figure 9 Na⁺/H⁺ exchanger-1 (NHE-1) regulation of autophagy via Akt pathway. **(a, b)** Akt, pAkt, and the extent of light chain 3 (LC3) conversion were determined by western blot analysis of differentiated mouse podocyte cells (MPCs), **P*<0.01 vs tunicamycin (Tm) group, #*P*<0.01 vs Tm + pcDNA-NHE-1. **(c, d)** Formation of acidic autophagic vacuoles (red granules) in differentiated MPCs cells is shown using acridine orange (AO). Acidic autophagic vacuoles were quantified, and data are presented as the number of red granules per cell. A minimum of 100 cells was counted, **P*<0.01 vs Tm group, #*P*<0.01 vs Tm + pcDNA-NHE-1. Cells were transiently transfected with pcDNA 3.1 vector (negative control) or pcDNA-NHE-1 vector for 38 h. Tm (2.5 μg/ml) with or without 50 nM wortmannin or 50 nM LY294002 was then added to cells for 10 h. This experiment was repeated three times. **(e, f)** Akt, the extent of LC3 conversion, and synaptopodin expression was determined by western blot analysis of differentiated MPCs under conditions of NHE-1 overexpression, transfected with non-targeted (con), or SignalSilence Akt small interfering RNA (siRNA) I (+), **P*<0.01 vs control. **(g, h)** Akt, the extents of LC3 conversion, and synaptopodin expression were determined by western blot analysis in differentiated MPCs under NHE-1 overexpression, transfected with non-targeted (con), or SignalSilenceATG-7 siRNA I (+), **P*<0.01 vs control. Data are representative of three independent experiments.

proteinuria. These changes resulted in podocyte loss and late-onset glomerulosclerosis. Further, Atg5 podocyte-specific knockout mice exhibited strongly increased susceptibility to models of glomerular disease. These findings highlight the importance of induced autophagy as a key homeostatic mechanism to maintain podocyte integrity. Our results in podocytes support this, as podocyte autophagy is an important supplementary mechanism of internal environmental adaptation. Therefore, regulation of autophagy activation might enhance the clearance of unfolded/misfolded proteins and reduce injury to podocytes.

NHE-1 is a critical plasma membrane protein that regulates cell survival and has a central role in the maintenance of intracellular volume and pH.^{38,39} In addition to the role of NHE-1 in electroneutral Na⁺/H⁺ transport, the NHE-1 cytosolic tail domain acts as a scaffold by binding with ezrin/radixin/moesin proteins^{24,40} and phosphatidylinositol 4,5-bisphosphate, which initiates the formation of a signaling complex that culminates in Akt activation and opposition to the initial apoptotic stress.⁴¹ Although this latter role has been elucidated in renal tubular epithelial cells *in vitro*, it is not well understood in podocytes. In the PHN rat model, we found that podocyte injury and proteinuria were accompanied by decreased NHE-1 expression. *In vitro*, we found that induction of ER stress proteins caused a reduction in NHE-1 expression. Furthermore, overexpression of NHE-1 has been shown to result in accumulated LC3 dot formation in the cytoplasm with no loss of synaptopodin after induction of ER stress. In contrast, NHE-1 deficiency inhibited GFP-LC3B dot formation and then aggravated the loss of synaptopodin and cell apoptosis. Here, we show for the first time that NHE-1 can protect podocytes from damage caused by environmental stress through autophagy activation. It is important to maintain the integrity of the cytoskeleton, stabilize the slit diaphragms of glomeruli, reduce the apoptosis, and decrease proteinuria. Another study suggested that the PI3K/Akt pathway has a key role in NHE-1 regulation of the cytoskeleton and cell survival.²³ In this study, we used siRNA-Akt and siRNA-ATG-7 to transfect MCP cells that overexpressed NHE-1. The results showed that siRNA-Akt interference blocked the protective effect due to NHE-1 and autophagy activity in podocytes. In addition, directly interfering with autophagy using ATG-7 siRNA

inhibited the protective effect due to NHE-1 but did not affect Akt levels. This result indicates that Akt is the upstream signaling pathway of autophagy, and NHE-1 could activate autophagy via Akt pathway.

On the basis of the above results, we speculate that NHE-1 expression is lower owing to podocyte cytoskeleton damage rather than a protective reduction during the process of PHN model, and the decreased expression of NHE-1 further aggravates the podocyte damage by downregulating autophagy in a vicious cycle. Therefore, NHE-1 regulation of autophagy might be considered another reparative mechanism that protects podocytes against environmental stress.

In summary, we showed that induction of ER stress in podocytes is an important cause of increased proteinuria *in vivo*. The efficiency of autophagy seems to include a system for degradation of proteins unfolded or misfolded due to ER stress. NHE-1 activates autophagy via Akt pathway and reduces ER stress-induced injury in podocytes, which is a novel pathway for prevention of podocyte injury and amelioration of proteinuria during the course of glomerular disease.

Supplementary Information accompanies the paper on the Laboratory Investigation website (<http://www.laboratoryinvestigation.org>)

ACKNOWLEDGMENTS

We thank Dr Peter Mundel for the generous gift of MPCs and Professor Tony Green for a gift of the full-length NHE-1 cDNA plasmid. This work was supported by grants from Programs of the National Basic Research Program of China (2011CB944000, 2013CB530800), the National Natural Science Foundation of China (30800521, 81070267), and the Major National S&T Program (2010ZX9102-204).

DISCLOSURE/CONFLICT OF INTEREST

The authors declare no conflict of interest.

1. Pavenstadt H, Kriz W, Kretzler M. Cell biology of the glomerular podocyte. *Physiol Rev* 2003;83:253–307.
2. Somlo S, Mundel P. Getting a foothold in nephrotic syndrome. *Nat Genet* 2000;24:333–335.
3. Endlich K, Kriz W, Witzgall R. Update in podocyte biology. *Curr Opin Nephrol Hypertens* 2001;10:331–340.
4. Eddy AA, Schnaper HW. The nephrotic syndrome: from the simple to the complex. *Semin Nephrol* 1998;18:304–316.
5. Cybulsky AV, Takano T, Papillon J, et al. Complement C5b-9 membrane attack complex increases expression of endoplasmic reticulum stress proteins in glomerular epithelial cells. *J Biol Chem* 2002;277:41342–41351.

6. Cybulsky AV, Takano T, Papillon J, *et al*. Role of the endoplasmic reticulum unfolded protein response in glomerular epithelial cell injury. *J Biol Chem* 2005;280:24396–24403.
7. Nakajo A, Khoshnoodi J, Takenaka H, *et al*. Mizoribine corrects defective nephrin biogenesis by restoring intracellular energy balance. *J Am Soc Nephrol* 2007;18:2554–2564.
8. Mori K. Tripartite management of unfolded proteins in the endoplasmic reticulum. *Cell* 2000;101:451–454.
9. Smoyer WE, Mundel P, Gupta A, *et al*. Podocyte alpha-actinin induction precedes foot process effacement in experimental nephrotic syndrome. *Am J Physiol* 1997;273(1 Pt 2):F150–F157.
10. Mizushima N, Ohsumi Y, Yoshimori T. Autophagosome formation in mammalian cells. *Cell Struct Funct* 2002;27:421–429.
11. Kroemer G, White E. Autophagy for the avoidance of degenerative, inflammatory, infectious, and neoplastic disease. *Curr Opin Cell Biol* 2010;22:121–123.
12. Mizushima N, Levine B, Cuervo AM, *et al*. Autophagy fights disease through cellular self-digestion. *Nature* 2008;451:1069–1075.
13. Kuma A, Hatano M, Matsui M, *et al*. The role of autophagy during the early neonatal starvation period. *Nature* 2004;432:1032–1036.
14. Lum JJ, Bauer DE, Kong M, *et al*. Growth factor regulation of autophagy and cell survival in the absence of apoptosis. *Cell* 2005;120:237–248.
15. Asanuma K, Tanida I, Shirato I, *et al*. MAP-LC3, a promising autophagosomal marker, is processed during the differentiation and recovery of podocytes from PAN nephrosis. *FASEB J* 2003;17:1165–1167.
16. Mizushima N, Yamamoto A, Matsui M, *et al*. *In vivo* analysis of autophagy in response to nutrient starvation using transgenic mice expressing a fluorescent autophagosome marker. *Mol Biol Cell* 2004;15:1101–1111.
17. Sato S, Kitamura H, Adachi A, *et al*. Two types of autophagy in the podocytes in renal biopsy specimens: ultrastructural study. *J Submicrosc Cytol Pathol* 2006;38:167–174.
18. Ogata M, Hino SI, Saito A, *et al*. Autophagy is activated for cell survival after endoplasmic reticulum stress. *Mol Cell Biol* 2006;26:9220–9231.
19. Shimizu S, Kanaseki T, Mizushima N, *et al*. Role of Bcl-2 family proteins in a non-apoptotic programmed cell death dependent on autophagy genes. *Nat Cell Biol* 2004;6:1221–1228.
20. Bursch W. The autophagosomal-lysosomal compartment in programmed cell death. *Cell Death Differ* 2001;8:569–581.
21. Yu L, Alva A, Su H, *et al*. Regulation of an ATG7-beclin 1 program of autophagic cell death by caspase-8. *Science* 2004;304:1500–1502.
22. Coaxum SD, Garnovskaya MN, Gooz M, *et al*. Epidermal growth factor activates Na⁺/H⁺ exchanger in podocytes through a mechanism that involves Janus kinase and calmodulin. *Biochim Biophys Acta* 2009;1793:1174–1181.
23. Schelling JR, Abu Jawdeh BG. Regulation of cell survival by Na⁺/H⁺ exchanger-1. *Am J Physiol Renal Physiol* 2008;295:F625–F632.
24. Denker SP, Huang DC, Orlowski J, *et al*. Direct binding of the Na⁺-H⁺ exchanger NHE1 to ERM proteins regulates the cortical cytoskeleton and cell shape independently of H(+) translocation. *Mol Cell* 2000;6:1425–1436.
25. Periyasamy-Thandavan S, Jiang M, Schoenlein P, *et al*. Autophagy: molecular machinery, regulation, and implications for renal pathophysiology. *Am J Physiol Renal Physiol* 2009;297:F244–F256.
26. Salant DJ, Cybulsky AV. Experimental glomerulonephritis. *Methods Enzymol* 1988;162:421–461.
27. Mundel P, Reiser J, Zuniga Mejia Borja A, *et al*. Rearrangements of the cytoskeleton and cell contacts induce process formation during differentiation of conditionally immortalized mouse podocyte cell lines. *Exp Cell Res* 1997;236:248–258.
28. Hartleben B, Godel M, Meyer-Schwesinger C, *et al*. Autophagy influences glomerular disease susceptibility and maintains podocyte homeostasis in aging mice. *J Clin Invest* 2010;120:1084–1096.
29. Kabeya Y, Mizushima N, Ueno T, *et al*. LC3, a mammalian homologue of yeast Apg8p, is localized in autophagosome membranes after processing. *EMBO J* 2000;19:5720–5728.
30. Ohsumi Y, Mizushima N. Two ubiquitin-like conjugation systems essential for autophagy. *Semin Cell Dev Biol* 2004;15:231–236.
31. Klionsky DJ, Abdalla FC, Abeliovich H, *et al*. Guidelines for the use and interpretation of assays for monitoring autophagy. *Autophagy* 2012;8:445–544.
32. Petiot A, Ougier-Denis E, Blommaert EF, *et al*. Distinct classes of phosphatidylinositol 3'-kinases are involved in signaling pathways that control macroautophagy in HT-29 cells. *J Biol Chem* 2000;275:992–998.
33. D'Agati VD. Podocyte injury in focal segmental glomerulosclerosis: Lessons from animal models (a play in five acts). *Kidney Int* 2008;73:399–406.
34. Hegde RS, Ploegh HL. Quality and quantity control at the endoplasmic reticulum. *Curr Opin Cell Biol* 2010;22:437–446.
35. Cybulsky AV. Endoplasmic reticulum stress in proteinuric kidney disease. *Kidney Int* 2010;77:187–193.
36. Saran AM, Yuan H, Takeuchi E, *et al*. Complement mediates nephrin redistribution and actin dissociation in experimental membranous nephropathy. *Kidney Int* 2003;64:2072–2078.
37. Kitamura M. Endoplasmic reticulum stress and unfolded protein response in renal pathophysiology: janus faces. *Am J Physiol Renal Physiol* 2008;295:F323–F334.
38. Bianchini L, Kapus A, Lukacs G, *et al*. Responsiveness of mutants of NHE1 isoform of Na⁺/H⁺ antiporter to osmotic stress. *Am J Physiol* 1995;269(4 Pt 1):C998–1007.
39. Thompson CB. Apoptosis in the pathogenesis and treatment of disease. *Science* 1995;267:1456–1462.
40. Denker SP, Barber DL. Ion transport proteins anchor and regulate the cytoskeleton. *Curr Opin Cell Biol* 2002;14:214–220.
41. Wu KL, Khan S, Lakhe-Reddy S, *et al*. The NHE1 Na⁺/H⁺ exchanger recruits ezrin/radixin/moesin proteins to regulate Akt-dependent cell survival. *J Biol Chem* 2004;279:26280–26286.